Chemical Engineering Journal 152 (2009) 339–346

Contents lists available at ScienceDirect

Chemical Engineering Journal

journal homepage: www.elsevier.com/locate/cej

Adsorption kinetics and thermodynamic parameters of cationic dyes from aqueous solutions by using a new strong cation-exchange resin

Gulay Bayramoglu*, Begum Altintas, M. Yakup Arica

Biochemical Processing and Biomaterial Research Laboratory, Faculty of Arts and Sciences, Gazi University, Teknik Okullar, 06500 Ankara, Turkey

ARTICLE INFO

Article history:
Received 1 February 2009
Received in revised form 20 April 2009
Accepted 21 April 2009

Keywords:
SI-ATRP
Cation exchanger
Adsorption
Basic dyes
Isotherms
Kinetics

ABSTRACT

Poly(glycidylmethacrylate) was grafted via surface-initiated-atom transfer radical polymerization (SI-ATRP) on a cross-linked acrylate based resin. Epoxy groups of the grafted polymer, were modified into strong cation-exchange groups (i.e., sulfonic groups) in the presence of sodium sulfite. The adsorption of Crystal Violet and Basic Fuchsine on the strong cation-exchange resin was studied under different experimental conditions. The adsorption process for both basic dyes was pH dependent. The maximum adsorption was observed for both dyes between pH 2.0 and 7.0. The maximum adsorption capacity of the cation-exchange resin for CV and BF dyes were found to be 76.8 and 127.0 mg/g, respectively. Adsorption of the dyes on the resin fitted to Langmuir and Temkin isotherm models and followed the pseudo-second-order kinetics. The values of Gibbs free energy of adsorption (ΔG°) were found to be −2.92 and −6.31 kJ/mol at 308 K for CV and BF dyes, respectively. These negative values indicated the spontaneity of the adsorption of the dyes on the resin. Desorption of both dyes was achieved from the resin by using 0.1 M HNO_3 and desorption ratio up to 97% was obtained over seven adsorption/desorption cycles.

1. Introduction

Dyes are present in the wastewater streams of many industrial sectors such as, dyeing, textile, tannery and the paint industry. The dye molecules or their metabolites (e.g., aromatic amines) may be highly toxic, potentially carcinogenic, mutagenic and allergenic on exposed organisms. They contaminate not only the environment but also traverse through the entire food chain, leading to biomagnification [1–5]. There are about 3000 types of dyes in the world market. Among them, cationic dyes are more toxic than anionic dyes, and their tinctorial values are very high (less than 1.0 mg/L) [5]. Cationic dyes can easily interact with negatively charged cells membrane surfaces, and can enter in to cells and concentrate in the cytoplasma [6]. Crystal Violet and Basic Fuchsine are cationic dyes, and extensively used in textile dyeing and paper printing [7,8]. A range of conventional physico-chemical and biological treatment technologies for dye removal from the wastewater have been investigated extensively. Among them, adsorption has been found to be superior to other techniques for dye wastewater treatment in terms of cost, simplicity of design, ease of operation and insensitivity to toxic substances [9–16]. Many solid materials as adsorbents have been investigated, which include activated carbons, alginate, chitosan and modified chitosan, functionalized polymeric resins. The later resins have been employed as an excellent adsorbent for sorption of phenols [17,18], textile dyes [19,20], enzymes [21], and in pollution control, as a chelating adsorbent for binding harmful metal ions [22–24].

In recent years, the fibrous polymer grafted and functionalized resin have been used increasingly as an alternative to activated carbon and other adsorbents due to their economic feasibility, adsorption-regeneration properties and mechanical strength [25,26]. Such material is characterized by large surface areas, narrow size distribution and a moderate swelling character, and can be easily adapted to various continuous reactor applications for treatment of wastewaters. Recently, a strong cation-exchange membrane has been used to adsorb a basic dye (i.e., Methyl Violet 2B) from wastewater and is proven to be an effective adsorbent for the removal of the basic dyes [27]. The surface modification is very helpful in the improvement of the adsorption capacity and selectivity of the resin by taking advantage of specific interactions between the adsorbents and the target molecules [28–30]. Furthermore, the application of polymeric resins for the removal of dyes from the aqueous medium is not well documented, and efficient adsorbents for removal of textile dyes still remain to be developed. In this study, fibrous polymer grafted and acidic sulfonic groups functionalized resin have been used first time to remove cationic dyes viz. Crystal Violet and Basic Fuchsine from aqueous solutions. These dyes were selected because they are widely used in Turkey textile dyeing industry and have high tinctorial values: even a concentration as low as 1.0 mg/L produces a distinct color. The effects of solution pH, contact time, adsorbent dosage, adsorbent concentration, reac-

* Corresponding author. Tel.: +90 312 202 1142; fax: +90 312 212 2279.
E-mail addresses: g_bayramoglu@hotmail.com, gbayramoglu@gazi.edu.tr (G. Bayramoglu), yakuparica@tnn.net (M.Y. Arica).

1385-8947/$ – see front matter © 2009 Elsevier B.V. All rights reserved.
doi:10.1016/j.cej.2009.04.051

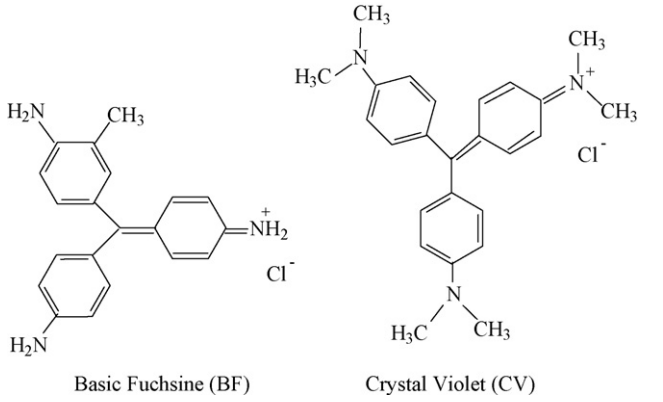

Fig. 1. The chemical structures of Crystal Violet (CV) (A) and Basic Fuchsine (BF) (B).

tion temperature, and ionic strength on the dyes removal efficiency of the resin were studied. Adsorption isotherms, kinetics and thermodynamic parameters were also evaluated for adsorption of both dyes on the cation-exchange resin.

2. Materials and methods

2.1. Materials

Bipyridine, CuBr, 2-bromo-2-methylpropionyl bromide, triethylamine, tetrahydrofuran, aqueous ammonia α,α′-azobisizobutyronitrile (AIBN), Crystal Violet (CV) and Basic Fuchsine (BF) were obtained from Sigma–Aldrich (St. Louis, USA). The monomers, 2-hydroxyethyl methacrylate (HEMA), glycidyl methacrylate (GMA) and ethyleneglycol dimethacrylate (EGDMA) were supplied from Sigma–Aldrich. Both former monomers distilled under reduced pressure in the presence of an inhibitor (hydroquinone) and stored at 4 °C until use. All other chemicals were of analytical grade and were purchased from Merck (Darmstadt, Germany). The water used in the present work was purified using a Barnstead (Dubuque, IA, USA) ROpure LP reverse osmosis unit with a high flow cellulose acetate resin (Barnstead D2731) system. The chemical structures and properties of CV and BF dyes are presented in Fig. 1 and Table 1.

2.2. Preparation of Br-end surface resin

The cross-linked poly(hydroxyethylmethacrylate) resin was produced by suspension polymerization, and the method was described in detail elsewhere [31]. For Br-end functionalization, the cross-linked acrylate based resin (about 10.0 g), tetrahydrofuran (100 mL) and triethylamine (3.0 mL) were transferred into a round bottom flask, and it was stirred magnetically at 50 rpm. It was then 2-bromo-2-methylpropionyl bromide (2.0 mL) was added drop wise within 30 min. The bromination reaction was allowed to proceed for 5 h at room temperature. After the bromination reaction, the resin was removed, and extensively washed with acetone and purified water. The resin was dried in a vacuum oven for 1 day prior to grafting as reported previously [31]. Grafting of glycidyl methacrylate (GMA) on the Br-end functionalized resin was achieved via SI-ATRP. A 10 g Br-end functionalized resin was transferred into a glass reactor. The chemicals GMA (30 mL, 225 mmol), CuBr (0.6 g), bipyridine (2.81 g, 18.0 mmol) and dioxane (30 mL) were added. The solution was purged with nitrogen about 10 min, and the system was sealed and agitated magnetically. SI-ATRP reaction was carried out at 65 °C for 18 h. Then, the reaction content was transferred into acetone (250 mL) and stirred magnetically to remove polymerization impurities. The p(GMA) grafted resins were cleaned, and epoxy groups were modified in to sulfonic acid groups as previously reported [32].

Table 1
The general characteristics of Crystal Violet and Basic Fuchsine.

	Crystal Violet	Basic Fuchsine
Chemical formula	$C_{25}H_{30}ClN_3$	$C_{20}H_{20}ClN_3$
Molecular weight (g/mol)	407.99	337.86
C.I. number	42555	42510
λ_{max} (nm)	585	550

2.3. Characterization of ion-exchange resin

The grafting percentage (GP) was determined by calculating the percentage increase in weight using following equation:

$$GP(\%) = \left[\frac{m_{gf} - m_o}{m_o}\right] \times 100 \quad (1)$$

where m_o and m_{gf} are the weights of the resin before and after grafting, respectively.

The amount of available surface functional epoxy groups content of the resin was determined by pyridine–HCl method as described previously [33]. The content of sulfonic group grafted polymer chains was measured by titration against a standard potassium hydroxide solution (0.1N) using phenolphthalein as an indicator. The resins were coated with a thin layer of gold under reduced pressure and their scanning electron micrographs were obtained using a JEOL (JSM 5600) scanning electron microscope.

The FTIR spectra of the p(HEMA-g-GMA) and sulfonic acid functionalized resins were obtained by using a FTIR spectrophotometer (FT-IR 8000 Series, Shimadzu, Japan). The dry sample (about 0.01 g) mixed with KBr (0.1 g) and pressed into a tablet form. The FTIR spectrum was then recorded. The swelling ratio of the p(HEMA-g-GMA) and sulfonic acid functionalized resin was determined using a volumetric cylinder. The height of the dry resin (H_d) was measured and then purified water was added into the volumetric cylinder and mixed at 50 rpm for 24 h. Then, the height of the swollen resin (H_s) was recorded. The swelling ratio was determined by the following equation:

$$\text{Equilibrium water swelling ratio} = \frac{H_s}{H_d} \quad (2)$$

2.4. Adsorption studies

The adsorption of basic dyes on the cation-exchange resin was investigated in a batch system. Solutions of the dye, containing 25–700 mg/L, were prepared in purified water. The ranges of concentrations of each dye were prepared from stock solutions. Adsorption experiments were performed by agitating magnetically at 150 rpm, at 25 ± 2 °C for 2 h. The adsorption volume was 50 mL and a 50 mg resin was used in each test. After centrifugation, the amounts of unadsorbed dye in supernatant solutions were analyzed for its dye concentration using a double beam UV–vis spectrophotometer (Shimadzu, Tokyo, Japan; Model 1601). All measurements were made at 585 and 550 nm for Crystal Violet and Basic Fuchsine, respectively. The amount of adsorbed dye per gram cation-exchange resin (mg dye/g dry resin) was obtained by using the following expression [13],

$$q = \frac{(C_0 - C)V}{m} \quad (3)$$

where C_0 and C are the concentrations of dye in the solution before and after the adsorption in mg/L, respectively. q is the amount of dye sorbed onto a unit dry mass of the cation-exchange resin in mg/g, V is the volume of the dye solution in L, and m is the weight of the dry cation-exchange resin in g.

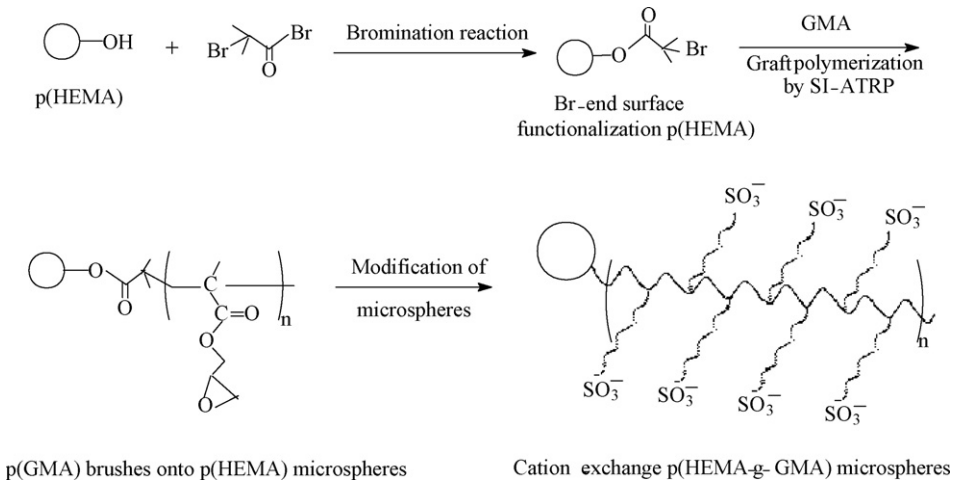

Fig. 2. Schematic representation of experimental protocols.

The effect of medium pH on the adsorption capacity of the cation-exchange resin was investigated in the pH range 2.0–9.0 for both dyes at 25 °C. To optimize the solid/liquid ratio (g/L) in terms of cost effect, batch experiments were conducted using different amounts of resin between 0.20 and 2.0 g/L resin at pH 5.0 and 25 °C. Sodium chloride (NaCl) was employed as background electrolyte changed between 0.0 and 1.0 M to investigate the influence of ionic strength on the dye removal. The effect of temperature was studied at four different temperatures (i.e., 15, 25, 35 and 45 °C) at pH 5.0. To determine the effect of initial concentrations of the dye on the adsorption rate and capacity on the cation-exchange resin, the initial concentration of each dye was varied between 25 and 700 mg/L in the adsorption medium at pH 5.0. For each adsorption experiments, the average of three replicates was reported.

3. Results and discussion

3.1. Properties of p(HEMA-g-GMA) resin

The successful use of SI-ATRP in controlled polymerization of hydrophilic monomers in aqueous media under mild conditions has recently opened up a new pathway for surface-initiated grafting of hydrophilic monomers [34,35]. Using ATRP, fibrous polymer chains on the polymer surface can be created to produce a materials surface with greater uniformity and flexibility (Fig. 2). In this study, the grafting percentage of p(GMA) is increased with the grafting time from 2 to 12 h, and leads to an increase up to 96% in grafting efficiency on the p(HEMA) resin (data not shown). The amount of available epoxy groups on the p(HEMA-g-GMA) resin surface was determined by HCl–pyridine method and was found to be 6.47 mmol/g resin. The epoxy groups of the resin were modified into sulfonic groups using Na_2SO_3 in alcohols/water. Following sulfonation reaction, the sulfonic group content of the resin was determined as 5.61 mmol/g support from the potentiometric titration. Thus, the cationic sulfonic groups could adsorb basic dyes with strong cation-exchange interactions (Fig. 2).

The resin is grafted with p(GMA) as proved by FTIR-spectroscopy (data not shown). The FTIR spectra of p(HEMA-g-GMA) have the characteristic stretching vibration band of hydrogen bounded alcohol of HEMA at ~3500 cm^{-1}. Among the characteristic vibrations of both HEMA and GMA are the methylene vibration at ~2980 cm^{-1} and the methyl vibration at 2920 cm^{-1}. The vibration at 1740 cm^{-1} represents the ester configuration of both HEMA and GMA. The FTIR spectra of the resin after sulfonation reaction have some absorption bands different from those of the p(HEMA)-g-p(GMA) resin. The most important absorption bands at 1030 and 1095 cm^{-1} representing symmetric and asymmetric stretching of sulfonate groups is due to the sulfonic groups formed during sulfonation reaction on the p(HEMA-g-GMA) resin. The stretching frequency band at 920 cm^{-1} is attributed to the S=O bond. The band at 1385 cm^{-1} is characteristic of the S=O stretching vibrations of undissociated sulfonic acid groups.

The surface morphology of the grafted resin was investigated by SEM. A representative micrograph is presented in Fig. 3. The surfaces of the p(HEMA-g-GMA) resin were smooth and nonporous. The fibrous polymer grafted supports can be suitable matrices due to their intrinsically high specific surface area. Thus, the grafted polymer can provide a high quantity binding sites for high adsorption capacity [28].

The swelling ratios of p(HEMA-g-GMA) and sulfonic acid functionalized resin were determined in purified water. When compared p(HEMA-g-GMA) resin (48%) with sulfonic acid modified counterpart, the swelling ratio of sulfonic group modified resin was increased to 98%. This appears reasonable when it is remembered that p(HEMA-g-GMA) is not highly polar compound and does not have fixed net charge. The sulfonic groups of grafted polymer chains introduced negative charges on the polymer structure, and should be caused more water uptake.

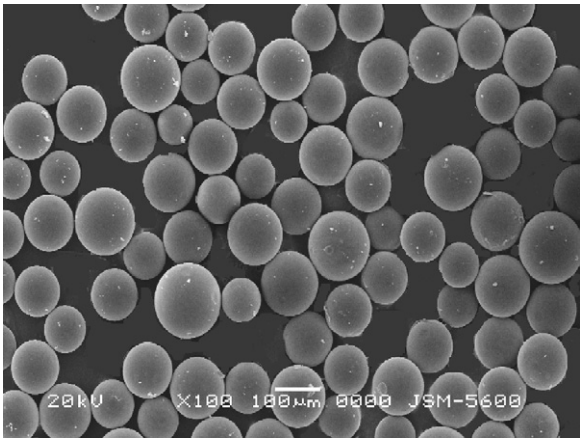

Fig. 3. SEM micrograph of cation-exchange resin.

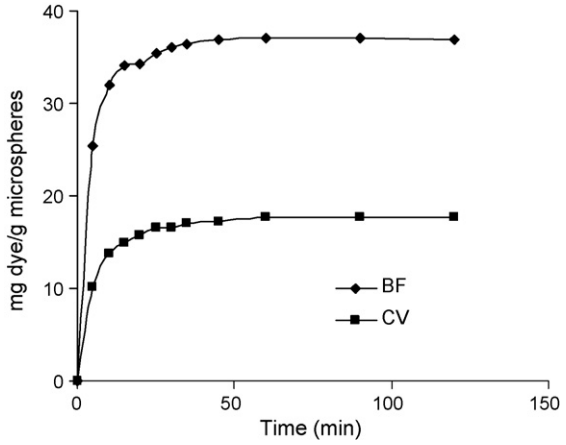

Fig. 4. Equilibrium adsorption time of CV and BF dyes on the cation-exchange resin. Adsorption conditions—initial concentration of dyes: 50 mg/L; medium pH: 5.0; solution volume: 50 mL; amount of cation-exchange resin: 1.0 g/L; temperature: 25 °C.

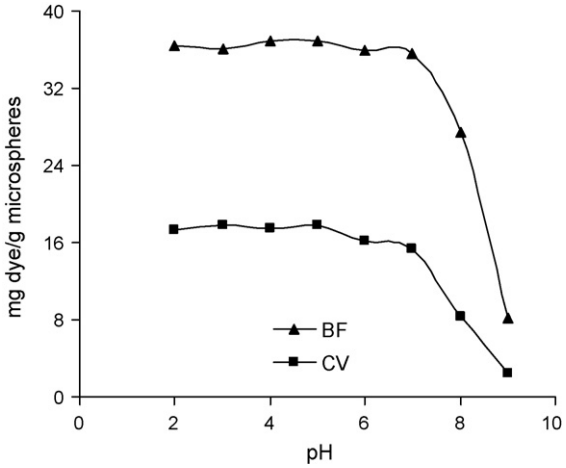

Fig. 6. Effect of pH's on the adsorption capacity of the cation-exchange resin for CV and BF basic dyes. Dye concentration: 50 mg/mL; temperature: 25 °C; solution volume: 50 mL; amount of cation-exchange resin: 1.0 g/L; adsorption time: 2 h.

3.2. Effect of adsorption system parameters

3.2.1. Contact time

The equilibrium adsorption time of two different basic dyes (i.e., CV and BF) on the sulfonic acid groups modified cation-exchange resin was investigated in 2 h. As seen in Fig. 4, a high initial slope for the adsorption curves is observed. It indicates that the initial uptake is rapid. This may be due to the fact that at the beginning of the sorption process all the reaction sites are vacant and hence the extent of removal is high. After a rapid initial uptake, there was a transitional phase in which the rate of uptake was slow with uptake reaching almost a constant value. Consequently, the adsorption of dyes was carried out in two distinct stages, a relatively rapid one followed by a slower one.

3.2.2. Effect of adsorbent dosage

The dependence of dye adsorption on adsorbent dosage was studied by varying the amount of adsorbents in the medium from 0.20 to 2.0 g/L while keeping other parameters constant such as initial concentration of dyes (50 mg/L), pH 5.0, stirring rate 150 rpm and contact time 2 h. As seen in Fig. 5, the removal efficiency of the adsorbent improved with increasing dose. This is expected due to the fact that the higher dose of adsorbents in the adsorption medium, the greater availability of exchangeable sites for the ions. The adsorption capacities of CV and BF basic dyes on the cation-exchange resin increased from 10.3 to 18.0 mg/g and 16.5 to 38.0 mg/g, respectively, with an increase in adsorbent concentration from 0.20 to 2.0 g/L. As the adsorbent dose increases, surface area and available sites for the dye molecules also increase, and consequently better adsorption takes place. Thus, the adsorption capacity of both dyes increased with the increase in the adsorbent dosage and reached an equilibrium value around 1.0 g of adsorbent dosage (Fig. 5). Therefore, the remaining experiments were carried out with 1.0 g resin/L.

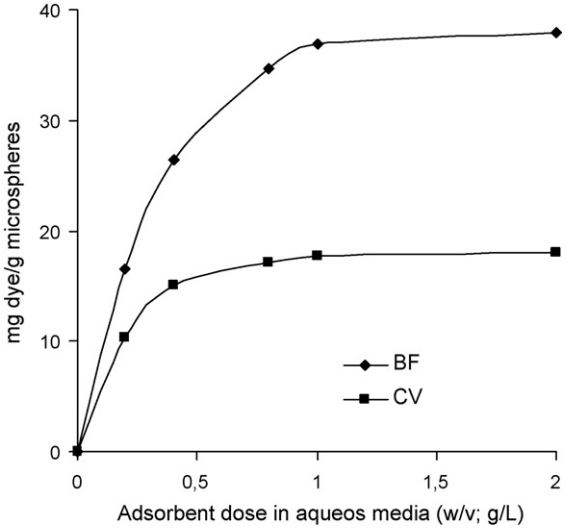

Fig. 5. Effect of resin dosage on the CV and BF dyes adsorption. Adsorption conditions—initial concentration of dyes: 50 mg/L; medium pH: 5.0; solution volume: 50 mL; amount of cation-exchange resin: 0.2–2.0 g/L; temperature: 25 °C.

3.2.3. Effect of pH and ionic strength

The adsorption of CV and BF basic dyes from aqueous solution onto cation-exchange resin is primarily influenced by the surface charge of the adsorbent and the degree of ionization of the adsorptive sites [3]. The effect of pH on the adsorption capacity of the cation-exchange resin was tested with two different basic dyes in the pH range of 2.0–9.0. As seen in Fig. 6, the removal efficiency of CV and BF dyes considered in this study remained almost constant in the pH range from 2.0 to 7.0. As expected, cationic functional groups of the tested basic dyes (i.e., CV and BF) did not interact with ion-exchange resin at pH higher than 8.0 due to the deprotonation of interactive primary and secondary amino groups of the dyes molecules. At pH 9.0, the adsorption capacity was very low due to weak electrostatic interactions between both dyes and sulfonic groups of the resin.

Sodium chloride is currently used in textile dyeing processes as it promotes the adsorption of the dyes by the textile fibers. Fig. 7 shows, the influence of the presence of NaCl on the adsorption capacity of the cation-exchange resin for both dyes. Addition of NaCl produced an important decrease of the performance of the resin for both dyes. As seen in this figure, the sorption capacity of the adsorbent depended on the ionic strength of the solution. When the ionic strength was increased, the electrical double layer surrounding the adsorbent surface was compressed and correspondingly resulted in a decrease in Crystal Violet and Basic Fucshine adsorption on to the cation-exchange resin.

3.2.4. Effect of initial concentrations of dyes on the adsorption efficiency

The initial dyes concentration provides an important driving force to overcome all mass transfer resistances of the dye molecules

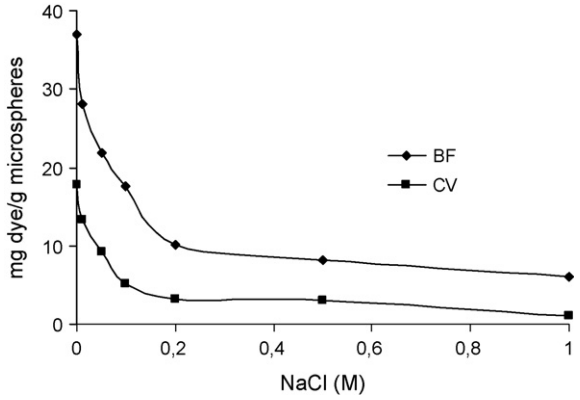

Fig. 7. Effect of NaCl concentration on the adsorption capacity of the cation-exchange resin for the basic dyes. Dye concentration: 50 mg/mL; temperature: 25 °C; medium pH: 5.0; solution volume: 50 mL; amount of cation-exchange resin: 1.0 g/L; adsorption time: 2 h.

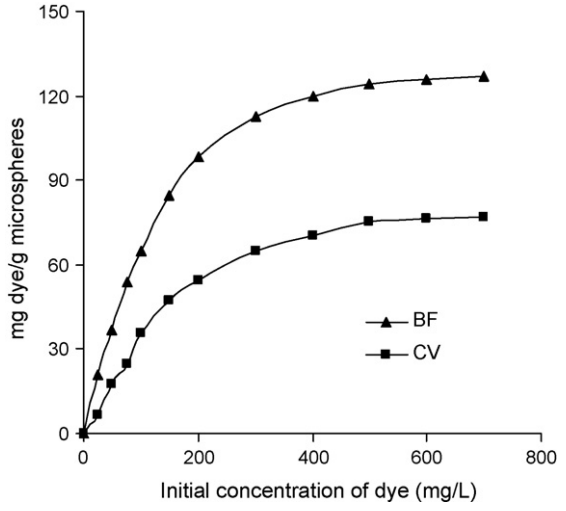

Fig. 8. Effect of initial concentration of the basic dye on the adsorption capacity of cation-exchange resin. Temperature: 25 °C; medium pH: 5.0; solution volume: 50 mL; amount of cation-exchange resin: 1.0 g/L; adsorption time: 2 h.

between the aqueous and solid phases. Hence, a higher initial concentration of dye will enhance the adsorption process. It should be noted that the initial dye concentration on an effluent was important since a given mass of the adsorbent can adsorb only a fixed amount of dye. The experimental equilibrium adsorption isotherms of both CV and BF basic dyes onto the cation-exchange resin were presented in Fig. 8. The maximum adsorption capacity of the resin was found to be 76.8 mg/g (0.188 mmol/g) for CV, and 127.0 mg/g (0.376 mmol/g) for BF at 25 °C. On the other hand, the data showed that as the initial concentration of each the dye increased from 25 to 700 mg/L, the percentage adsorption decreased from 35% to 11% for CV, and 74% to 18% for BF. This result showed that dye removal was highly concentration dependent [36]. It should be noted that the differences in adsorption capacity of resin for two different basic dyes should be caused by the chemical properties. Basic Fuchsine has a high adsorption capacity or reactivity towards to cation-exchange resin. The high adsorption capacity for BF dye may be resulted from the pendant primary amino groups of the dye molecules. In contrast, Crystal Violet molecule does not contain pendant amino groups; the two-methyl groups mask its each amino group.

3.3. Kinetic parameters

The kinetics of adsorption is important from the point of view that it controls the process efficiency. In order to examine the controlling mechanism of biosorption process such as mass transfer and chemical reaction, kinetic models were used to test the experimental data. The kinetics of dye adsorption on the cation-exchange resin was determined with three different kinetic models, i.e., the first- and second-order and the intra-particle diffusion model. The first-order rate equation of Lagergren is one of the most widely used equations for the sorption of solute from a liquid solution [37,38]. For this model, the following relation was used for the variation of adsorbed concentration with respect to time.

$$\log\left(\frac{q_{eq}}{q_{eq}-q_t}\right) = \frac{k_1 \cdot t}{2.303} \quad (4)$$

where k_1 is the rate constant of pseudo-first-order adsorption (min^{-1}) and q_{eq} and q_t denote the amounts of adsorption at equilibrium and at time t (mg/g), respectively. The slopes and intercepts of plots of $\log(q_{eq} - q_t)$ versus t were used to determine the pseudo-first-order rate constant k_1 and q_e.

In addition, a pseudo-second-order equation based on sorption equilibrium capacity may be expressed in the form [13]:

$$\frac{1}{q_t} = \frac{1}{k_2 q_{eq} t} + \frac{1}{q_{eq}} \quad (5)$$

where k_2 (g/(mg min)) is the rate constant of pseudo-second-order adsorption. The rate constant (k_2) and adsorption at equilibrium (q_{eq}) can be obtained from the intercept and slope, respectively, and there is no need to know any parameter beforehand.

According to experimental and theoretical kinetic data in Table 2, the experimental results obtained for the adsorption of CV and BF basic dyes on cation-exchange resin at optimum conditions of pH, contact time and dose of adsorbent were found to obey the second-order kinetic. The theoretical q_{eq} values estimated from the first-order kinetic model gave significantly different values compared to experimental values, and the correlation coefficients were also found to be lower. These results showed that the first-order kinetic model did not describe these sorption systems. The theoretical q_{eq} values for the resin were very close to the experimental

Table 2
The first- and second-order kinetics and intra-particle diffusion models for adsorption of CV and BF on the cation-exchange resin.

Dye	Temperature (K)	First-order		Second-order			Intra-particle diffusion		
		k_1 (min^{-1})	q_{eq} (mg/g)	R^2	k_2 (g/(mg min))	q_{eq} (mg/g)	R^2	K_i mg/(g $min^{0.5}$)	R^2
CV	288	0.166	69.68	0.986	0.216	52.63	0.990	1.85	0.725
	298	0.077	42.66	0.991	0.246	81.30	0.996	2.96	0.810
	308	0.173	75.85	0.987	0.297	90.91	0.998	3.25	0.847
	318	0.067	43.65	0.998	0.376	109.89	0.995	2.89	0.759
BF	288	0.196	162.18	0.961	0.278	111.10	0.989	3.27	0.712
	298	0.115	117.49	0.995	0.311	133.33	0.995	4.09	0.766
	308	0.059	33.81	0.970	0.582	144.96	0.998	3.14	0.805
	318	0.118	41.69	0.984	0.826	175.43	0.990	2.43	0.690

Table 3
Isotherm models constants and correlation coefficients for adsorption of Crystal Violet (CV) and Basic Fuchsine (BF) from aqueous solution.

Dye (K)	q_{exp} (mg/g)	Freundlich model			Langmuir model					Temkin model		
		n (g/L)	K_F (mg/g)	R^2	$b \times 10^2$ (L/mg)	Q_{max} (mg/g)	R^2	ΔG (kJ/mol)	R_L[a]	$K_T \times 10^2$ (L/mg)	B	R^2
CV												
288	48.4	1.63	1.21	0.948	0.62	62.5	0.990	−2.20	0.189	6.78	13.7	0.988
298	76.8	1.66	2.11	0.938	0.69	98.0	0.988	−2.56	0.172	7.85	21.1	0.993
308	88.3	1.78	2.99	0.965	0.77	108.7	0.998	−2.92	0.157	8.53	23.2	0.996
318	104.9	1.82	4.08	0.953	0.95	125.0	0.996	−3.59	0.131	10.29	27.1	0.991
BF												
288	102.6	2.45	9.21	0.975	1.79	113.7	0.996	−4.32	0.074	2.27	22.3	0.986
298	127.0	2.80	16.09	0.968	2.97	134.1	0.999	−5.72	0.046	5.02	23.6	0.993
308	143.4	2.78	18.80	0.969	3.49	151.3	0.998	−6.31	0.039	6.15	26.1	0.986
318	171.1	3.42	31.50	0.957	4.63	178.6	0.998	−7.28	0.029	25.6	24.1	0.934

[a] Initial concentrations (C_0) of CV and BF, 700 mg/L.

q_{eq} values in the case of second-order kinetics. The correlation coefficients for the linear plots of $1/q_t$ against $1/t$ for the second-order equation are greater than 0.989 for CV and BF dyes for contact times of 2 h. The pseudo-second-order equation at different temperature fitted well with the experimental data for two basic dyes (Table 2). The pseudo-second-order model is based on the assumption that the rate-determining step may be a chemical sorption involving valence forces through sharing or exchange of electrons between adsorbent and sorbate [38].

In order to assess the nature of the diffusion process reasonable for the adsorption of dyes onto the resin attempts were made to calculate the pore diffusion coefficients. When the water sample is shaken, the dye molecules are transported to the solid phase by the intra-particle transport phenomenon. The intra-particle transport is supposed to be the rate-controlling step. The rate of particle transport through this mechanism is slower than adsorption on the exterior surface site of the adsorbent. The amount of adsorbed species can lead varies proportionately with a function of retention time. The intra-particle diffusion model was proposed by Weber and Morris [39], the initial rate of intra-particular diffusion is calculated by linearization of the curve $q = f(t^{0.5})$:

$$q = K_i t^{0.5} \tag{6}$$

where q (mg/g) is the amount of adsorbed dye on the resin at time t (s), and K_i is the diffusion coefficient in the solid (mg/g min$^{0.5}$). K_i has been determined by a plot $q = f(t^{0.5})$ taking account only of the initial period.

Plots of CV and BF amounts adsorbed, q_t versus time$^{0.5}$, are plotted for cation-exchange resin (data not shown). All the plots have the similar general features, initial linear portion followed by a plateau. The initial linear portion was attributed to the intra-particle diffusion. However, such a deviation of the straight line from the origin could likely be due to the difference in the rate of boundary layer diffusion in the initial stage of adsorption. Generally, the intercept of the plot of q_t versus time$^{0.5}$ gives an idea about boundary layer thickness, the larger the value of the intercept, the greater the boundary layer diffusion effect is. The values of intra-particle diffusion rate constant, K_i, are tabulated in Table 2. These results indicate that the dye molecules diffused quickly among the sorbents at the beginning of the adsorption process, and then intra-particle diffusion slowed down and stabilized. If the regression of q versus $t^{0.5}$ is linear and passes through the origin, then intra-particle diffusion is the sole rate-limiting step. The deviation of straight lines from the origin indicates that intra-particle transport is not the rate-limiting step.

3.4. Equilibrium adsorption isotherms

Equilibrium data, commonly known as adsorption isotherms, are the basic requirements for the design of adsorption systems. Obtaining equilibrium data for a specific adsorbate/adsorbent system can be performed experimentally, with a time-consuming procedure that is incompatible with the growing need for sorption systems design. Analysis of equilibrium data is important for developing an equation that can be used to compare different sorbents under different operational conditions and to design and optimize an operating procedure [29,30].

The equilibrium removal of dyes was mathematically expressed in terms of adsorption isotherms. Some isotherm equations have been tested in the present study, namely the Langmuir, Freundlich, Dubinin–Radushkevich (D–R) and Temkin isotherm models (Fig. 9). These equations are given below in order:

$$q = \frac{Q_{max} b C_{eq}}{1 + b C_{eq}} \tag{7}$$

$$q = K_F (C_{eq})^{1/n} \tag{8}$$

$$\ln\ q_{eq} = \ln q_m - K\varepsilon^2 \tag{9}$$

$$q_{eq} = B \ln K_T + B \ln C_{eq} \tag{10}$$

For the Langmuir Eq. (7); the constant b is related to the energy of adsorption, C_{eq} is the equilibrium concentration of the dye in solution Q is the amount of adsorbed dye on the adsorbent surface and the constant Q_{max} represents the maximum binding at the complete saturation of adsorbent binding sites. K_F and n are the Freundlich adsorption isotherm constants characteristic of the system (Eq. (8)). K_F and n are indicative of the extent of the adsorption and the degree of non-linearity between solution concentration and adsorption, respectively. In the Dubinin–Radushkevich (D–R) isotherm equation (Eq. (9)), K is the constant related to the mean

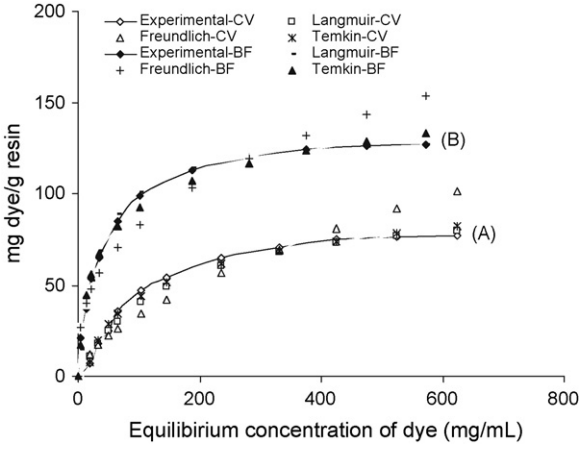

Fig. 9. Experimental, Langmuir, Freundlich and Temkin isotherms for adsorption of CV (A) and BF (B) dyes on the cation-exchange resin.

free energy of sorption, q_m is the theoretical saturation capacity, and ε is the Polanyi potential, equal to $RT\ln(1+(1/C_e))$. In Eq. (10), K_T and B are the Temkin isotherm constants. The isotherm constant K_T is the equilibrium binding constant (L/mg) corresponding to the maximum binding energy and constant B is related to the heat of adsorption (Temkin).

The results also showed that besides the Langmuir, Freundlich model and Temkin models are also suitable for describing the adsorptions of CV and BF basic dyes (Table 3). Among these isotherms, Freundlich isotherm was the poorest to fit the experimental adsorption equilibrium data (Fig. 9). Dubinin–Radushkevich (D–R) isotherm model has been used for the analysis of the dye adsorption on adsorbents. However, in this work, the corresponding semi-reciprocal isotherm plots ($\ln q_{eq}$ versus ε^2) of the experimental data gave a non-linear plot for the cation-exchange resin. The adsorptions of BF and CV basic dyes onto cation-exchange resin cannot be also described in terms of this model. Considering that Langmuir isotherm assumes a monolayer coverage and uniform activity distribution on the adsorbent surface, this is an expected result. Adsorption of CV and BF is quite a complex process, probably forming layers on the polymer chains. In addition, a variation of adsorption activity is expected with surface coverage. Both Langmuir and Temkin isotherms gave very good fit to the adsorption data of CV and BF on cation-exchange resin.

The essential features of a Langmuir isotherm can be expressed in terms of a dimensionless constant separation factor or equilibrium parameter, R_L, which is used to predict if an adsorption system is "favorable" or "unfavorable" [6,11].

$$R_L = \frac{1}{1+bC_0} \tag{11}$$

where C_0 is the initial metal concentration. The value of R_L indicates the shape of isotherm to be either unfavorable ($R_L > 1$) or linear ($R_L = 1$) or favorable ($0 < R_L < 1$) or irreversible ($R_L = 0$). Here, R_L values obtained for CV and BF dyes are listed in Table 3. The fact that all the R_L values for the adsorption of CV and BF onto ion-exchange resin are in the ranges of 0.189–0.131 and 0.074–0.029 at 288–318 K for 700 mg/L initial dye concentration, respectively and confirmed that the cation-exchange resin is favorable for adsorption of BF and CV dye under conditions studied (Table 3).

3.5. Thermodynamic parameters

Batch adsorption runs of basic dyes on cation-exchange resin were performed at different temperatures (15, 25, 35 and 45 °C), and the results are summarized for CV and BF dyes in Table 3. It is seen that the adsorption capacity increases with the increasing of the temperature, showing an endothermic adsorption process. Activation energy is determined according to the pseudo-second-order rate constant is expressed as a function of temperature by the Arrhenius equation, $k = A_o\exp(-E_a/RT)$. A_o, is the temperature independent factor, k is the second-order rate constant and R is the gas constant (8.314 J/(mol K)). Value of the activation energy, E_a, can be determined from the slope of $\ln k$ versus $1/T$ plot. The activation energies for BF and CV on the cation-exchange resin were calculated and the values were found to be 14.03 and 29.35 kJ/mol, respectively.

In order to evaluate the feasibility and the effect of temperature better, for dye adsorption onto cation-exchange resin, thermodynamic parameters such as standard free energy change (ΔG°), standard enthalpy change (ΔH°) and standard entropy change (ΔS°) were also obtained. The Gibbs free energy change of adsorption process was calculated by using the following equations:

$$\Delta G^\circ = -RT\ \ln K_a \tag{12}$$

where K_a is the dependency of the equilibrium association constant ($K_a = b$, from Langmuir constant). T is the solution temperature.

Standard enthalpy and entropy change values of adsorption can be calculated from van't Hoff equation given as below

$$\ln\ K_a = \frac{\Delta S^\circ}{R} - \frac{\Delta H^\circ}{RT} \tag{13}$$

The thermodynamic parameters, ΔG for both basic dyes adsorbed on the resin were calculated for each temperature and tabulated in Table 3. When the temperature increased from 288 to 318 K, ΔG is increased for both of CV and BF dyes. As presented in Table 3, the negative of ΔG values at given temperatures indicates the spontaneous nature of the adsorption and confirm the feasibility of the adsorption process. Generally, the change in adsorption enthalpy for physical adsorption is in the range of −20 to −40 kJ/mol, but chemisorption is between −400 and −80 kJ/mol. The enthalpy change values were obtained 10.71 and 24.39 kJ/mol for CV and BF, respectively. The positive value of ΔH° reveals the adsorption is endothermic and physical in nature. The enthalpy change value 10.71 and 24.39 kJ/mol indicates the uptake of CV and BF dyes on resin to be a physical adsorption. The adsorption enthalpy change for BF is larger than that of CV. It means the interaction between BF and cation-exchange resin surface is stronger and then leads to an enhanced adsorption. The entropy change values were obtained 44.66 and 99.27 J/(mol K) for CV and BF, respectively. Positive ΔS° values of CV and BF adsorption process indicates an irregular increase of the randomness at the cation-exchange resin–solution interface during adsorption.

3.6. Desorption and regeneration

The economic feasibility of using adsorbent to remove contaminants from wastewater relies on its regeneration ability during multiple adsorption/desorption cycles. In this study, we tested various desorption solutions in the batch system in order to find a suitable agent for basic dyes desorption from the cation-exchange resin and for cation-exchange resin regeneration. The optimal desorption condition for both dyes was 0.1 M HNO_3, and almost complete desorption (up to 98.7%) was achieved under this condition. These results indicate that CV and BF was bound onto the cation-exchange resin through a combination of electrostatic interactions. Seven adsorption desorption cycles were performed without significant decrease in adsorption capacity.

4. Conclusions

Adsorption process was shown to be highly efficient for color removal from wastewaters due to its sludge-free clean operation, simplicity and flexibility of design and complete removal of dyes even from dilute solutions. The result clearly demonstrated that cationic sulfonic groups contributed to the adsorption mechanism through electrostatic interactions between sulfonic groups of the adsorbent (which are known as strong cation exchangers) and the cationic sites of CV and BF basic dyes. The percentage uptake of dyes is concentration dependent, decreasing with an increase in dye concentration. The equilibrium adsorption behavior of CV and BF onto cation-exchange resin followed the Langmuir adsorption isotherm with a maximum theoretical adsorption capacity of 98.0 and 134.1 mg/g resin, respectively. The adsorption of both basic dyes on the cation-exchange resin was found to be mainly based on ion-exchange interactions, and these were confirmed by the results of adsorption isotherms. For the removal basic dyes from wastewater with the adsorption method, it is a promising route to graft functional polymer on the solid supports with high performance.

References

[1] G. Bayramoglu, M.Y. Arica, Kinetics of mercury ions removal from synthetic aqueous solutions using by novel magnetic p(GMA-MMA-EGDMA) beads, J. Hazard. Mater. 144 (2007) 449–457.

[2] G. Bayramoğlu, M.Y. Arıca, Biosorption of benzidine based textile dyes "Direct Blue 1 and Direct Red 128" using native and heat-treated biomass of *Trametes versicolor*, J. Hazard. Mater. 143 (2007) 135–143.

[3] S. Karcher, A. Kornmuller, M. Jekel, Anion exchange microspheres for removal of reactive dyes from textile wastewaters, Water Res. 36 (2002) 4717–4724.

[4] R.-Y. Lin, B.-S. Chen, G.-L. Chen, J.-Y. Wu, H.-C. Chiu, S.-Y. Suen, Preparation of porous PMMA/Na^+–montmorillonite cation-exchange membranes for cationic dye adsorption, J. Membr. Sci. 326 (2009) 117–129.

[5] G.S. Heiss, B. Gowan, E.R. Dabbs, Cloning of DNA from a *Rhodococcus* strain conferring the ability to decolorize sulfonated azo dyes, FEMS Microbiol. Lett. 99 (1992) 221–226.

[6] A.R. Oseroff, D. Ohuoha, G. Ara, D. McAuliffe, J. Foley, L. Cincotta, Intramitochondrial dyes allow selective in vitro photolysis of carcinoma cells, Proc. Natl. Acad. Sci. U.S.A. 88 (1986) 9729–9733.

[7] G.S. Gupta, S.P. Shukla, G. Prasad, V.N. Singh, China clay as an adsorbent for dye house wastewaters, Environ. Technol. 13 (1992) 925–936.

[8] R. Dhodapkar, N.N. Rao, S.P. Pande, T. Nandy, S. Devotta, Adsorption of cationic dyes on Jalshakti, super absorbent polymer and photocatalytic regeneration of the adsorbent, React. Funct. Polym. 67 (2007) 540–548.

[9] V.K. Garg, R. Kumar, R. Gupta, Removal of malachite green dye from aqueous solution by adsorption using agro-industry waste: a case study of *Prosopis cineraria*, Dyes Pigments 62 (2004) 1–10.

[10] V. Singh, A.K. Sharma, D.N. Tripathi, R. Sanghi, Poly(methylmethacrylate) grafted chitosan: an efficient adsorbent for anionic azo dyes, J. Hazard. Mater. 161 (2009) 955–966.

[11] Z. Aksu, A.I. Tatlı, Ö. Tunç, A comparative adsorption/biosorption study of Acid Blue 161: effect of temperature on equilibrium and kinetic parameters, Chem. Eng. J. 142 (2008) 23–39.

[12] M.S. Chiou, H.Y. Li, Adsorption behavior of reactive dye in aqueous solution on chemical cross-linked chitosan microspheres, Chemosphere 50 (2003) 1095–1105.

[13] M.Y. Arica, G. Bayramoglu, Biosorption of Reactive Red-120 dye from aqueous solution by native and modified fungus biomass preparations of *Lentinus sajor-caju*, J. Hazard. Mater. 149 (2007) 499–507.

[14] Z. Aksu, G. Karabayır, Comparison of biosorption properties of different kinds of fungi for the removal of Gryfalan Black RL metal-complex dye, Bioresour. Technol. 99 (2008) 7730–7741.

[15] S.V. Mohan, S.V. Ramanaiah, P.N. Sarma, Biosorption of direct azo dye from aqueous phase onto *Spirogyra* sp. I02: evaluation of kinetics and mechanistic aspects, Biochem. Eng. J. 38 (2008) 61–69.

[16] S.T. Akar, A. Gorgulu, Z. Kaynak, B. Anilan, T. Akar, Biosorption of Reactive Blue 49 dye under batch and continuous mode using a mixed biosorbent of macrofungus *Agaricus bisporus* and *Thuja orientalis* cones, Chem. Eng. J. 148 (2009) 26–34.

[17] C. Long, A. Li, H. Wu, Q. Zhang, Adsorption of naphthalene onto macroporous and hypercrosslinked polymeric adsorbent: effect of pore structure of adsorbents on thermodynamic and kinetic properties, Colloids Surf. A: Physicochem. Eng. Aspects 333 (2009) 150–155.

[18] X. Bai, B. Liu, J. Yan, Adsorption behavior of water-wettable hydrophobic porous resins based on divinylbenzene and methyl acrylate, React. Funct. Polym. 63 (2005) 43–53.

[19] V. Bekiari, M. Sotiropoulou, G. Bokias, P. Lianos, Use of poly(N,N-dimethylacrylamide-co-sodium acrylate) hydrogel to extract cationic dyes and metals from water, Colloids Surf. A: Physicochem. Eng. Aspects 312 (2008) 214–218.

[20] X.-F. Sun, S.-G. Wang, X.-W. Liu, W.-X. Gong, N. Bao, B.-Y. Gao, H.-Y. Zhang, Biosorption of malachite green from aqueous solutions onto aerobic granules: Kinetic and equilibrium studies, Bioresour. Technol. 99 (9) (2008) 3475–3483.

[21] G. Bayramoglu, M.Y. Arıca, Enzymatic removal of phenol and p-chlorophenol in enzyme reactor: horseradish peroxidase immobilized on magnetic beads, J. Hazard. Mater. 156 (2008) 148–155.

[22] G. Bayramoglu, M.Y. Arica, Adsorption of Cr(VI) onto PEI immobilized acrylate-based magnetic beads: isotherms, kinetics and thermodynamics study, Chem. Eng. J. 139 (2008) 20–28.

[23] B. Pan, B. Pan, W. Zhang, L. Lv, Q. Zhang, S. Zheng, Development of polymeric and polymer-based hybrid adsorbents for pollutants removal from waters, Chem. Eng. J. 151 (2009) 19–29.

[24] O. Genç, L. Soysal, G. Bayramoglu, M.Y. Arica, S. Bektas, Procion Green H-4G immobilized poly(2-hydroxyethylmethacrylate/chitosan) composite membranes for heavy metal removal, J. Hazard. Mater. 97 (2003) 111–125.

[25] S. Chatterjee, D.S. Lee, M.W. Lee, S.H. Woo, Enhanced adsorption of Congo red from aqueous solutions by chitosan hydrogel beads impregnated with cetyl trimethyl ammonium bromide, Bioresour. Technol. 100 (2009) 2803–2809.

[26] T.S. Anirudhan, P.S. Suchithra, P.G. Radhakrishnan, Synthesis and characterization of humic acid immobilized-polymer/bentonite composites and their ability to adsorb basic dyes from aqueous solutions, Appl. Clay Sci. 43 (2009) 336–342.

[27] J.-S. Wu, C.-H. Liu, K.H. Chu, S.-Y. Suen, Removal of cationic dye methyl violet 2B from water by cation exchange membranes, J. Membr. Sci. 309 (2008) 239–245.

[28] P. Liu, J. Guo, Polyacrylamide grafted attapulgite (PAM-ATP) via surface-initiated atom transfer radical polymerization (SI-ATRP) for removal of Hg(II) ion and dyes, Colloids Surf. A: Physicochem. Eng. Aspects 282–283 (2006) 498–503.

[29] G. Bayramoglu, S. Bektas, M.Y. Arica, Removal of Cd(II), Hg(II) and Pb(II) ions from aqueous solution using p(HEMA/chitosan) membranes, J. Appl. Polym. Sci. 106 (2007) 169–177.

[30] G. Bayramoğlu, M.Y. Arica, Ethylenediamine grafted poly(glycidylmethacrylate-co-methylmethacrylate) adsorbent for removal of chromate anions, Sep. Purif. Technol. 45 (2005) 192–199.

[31] M.Y. Arica, G. Bayramoglu, Synthesis and spectroscopic characterization of super paramagnetic beads of copolymers of methacrylic acid, methyl methacrylate and ethyleneglycol dimethacrylate and their application to protein separation, Polym. Int. 57 (2008) 70–76.

[32] G. Bayramoglu, M.Y. Arica, Preparation of and characterization of comb type polymer coated poly(HEMA/EGDMA) microspheres containing surface-anchored sulfonic acid: application in γ-globulin separation, React. Funct. Polym. 69 (2009) 189–196.

[33] S. Sidney, Quantitative Organic Analysis, 3rd ed., John Wiley and Sons, New York, 1967.

[34] B.-E. Wang, Y.-Y. Hu, Bioaccumulation versus adsorption of reactive dye by immobilized growing *Aspergillus fumigatus* beads, J. Hazard. Mater. 157 (2008) 1–7.

[35] J.H. Koh, Y.W. Kim, J.T. Park, B.R. Min, J.H. Kim, Nanofiltration membranes based on poly(vinylidene fluoride-co-chlorotrifluoroethylene)-graft-poly(styrene sulfonic acid), Polym. Adv. Technol. 19 (2008) 1643–1648.

[36] V.P. Vinod, T.S. Anirudhan, Adsorption behaviour of basic dyes on the humic acid immobilized pillared clay, Water Air Soil Pollut. 150 (2003) 193–217.

[37] S. Lagergren, Zur theorie der sogenannten adsorption gelöster stoffe, Kungliga Svenska Vetenskapsakademiens Handlingar 24 (1898) 1–39.

[38] Y.S. Ho, Second-order kinetic model for the sorption of cadmium onto tree fern: a comparison of linear and non-linear methods, Water Res. 40 (2006) 119–125.

[39] J.W.J. Weber, J.C. Morriss, Kinetics of adsorption on carbon from solution, J. Sanit. Eng. Div. Am. Soc. Civil Eng. 89 (1963) 31–60.